

Carbon Nanotube Reinforced Porous Gels of Poly(methyl methacrylate) with Nonsolvents as Porogens

Malvina Vaysse,[†] Mostafa Kamal Khan, and Pudupadi Sundararajan*

Department of Chemistry, Carleton University, 1125 Colonel By Drive, Ottawa, Ontario K1S 5B6, Canada.

[†] Student intern from Ecole Nationale Supérieure de Chimie de Montpellier, France. Current address: la lande sud, 24600 Saint Martin de Riberac, France

Received October 1, 2008. Revised Manuscript Received April 16, 2009

We fabricated porous organogels of poly(methyl methacrylate) (PMMA) using nonsolvents as porogens. In contrast to the use of inorganic materials, surfactants, etc., as porogens, we used the nonsolvents for PMMA such as water, methanol, propanol, and cyclohexane. This offers the advantage of not having to extract the porogen after gel formation. The nonsolvent simply evaporates. We find that the pore size can be controlled by matching the solubility parameters of the solvent/nonsolvent mixtures and that of PMMA. Incorporation of CNT itself does not lead to porous morphology in this case, unless a nonsolvent is added. Introducing carbon nanotubes during the addition of nonsolvent for gelation enhances the elongation ratio of the PMMA gel. We show that the CNT forms a network around the pores. Infrared and Raman spectra show no specific interaction between the CNT and PMMA. Hence, the former simply acts as a reinforcing filler.

Introduction

Polymeric porous structures are promising materials due to their potential applications in diverse areas such as catalysis, medical implants, superabsorbent materials, and separation processes.¹ From the point of view of supramolecular science, it is an interesting challenge to design polymer networks with a controlled porous architecture. On the basis of porous inorganic structures, porosity in polymeric systems is sometimes generated using phase inversion, foaming, spinning, and emulsion techniques. But most of these processes are not well developed for organic materials and lead to inhomogeneous macroporosity or involve long and complex manipulations.

Thermoreversible gels consist of physical polymer gels with a structure sensitive toward temperature variations. Studies of Keller² and Berghmans³ in 1990 established that the gelation of polystyrene and poly(methyl methacrylate) (PMMA) was due to liquid–liquid phase separation arrested by vitrification. Porous structures arising in such thermoreversible gelation depend on cooling rate, solvent system, etc.⁴ At present, phase separation and porogen techniques are the most developed to generate porosity.^{5,6} The latter involves dispersion of pore generators (e.g., surfactants, NaCl, PEG, sucrose) during the gelation which are extracted later with a suitable solvent. Other techniques involving gelation in the presence of water/oil emulsion⁷ and gas blowing⁸ have also been developed. Other examples of porous polymer films preparations are repeated freeze/dry process of the

poly(vinyl alcohol) melt to prepare porous hydrogel⁹ and cross-linking butyl rubber in frozen benzene.¹⁰

In this paper, we discuss the formation of porous gels of PMMA by the addition of a nonsolvent. Nonsolvents are used to cause phase inversion in polymer membrane science.¹¹ Essentially, the polymer film (prepared using a solvent) is immersed in a nonsolvent bath to cause coagulation and polymer precipitation. Lin et al.¹² found that during the preparation of PMMA membranes adding a small amount of water to the PMMA solution in *N*-methyl-2-pyrrolidone, casting the film, and using water as a coagulant prevented the formation of macrovoids. They attributed it to the gel formation in the film when water was added.

Apart from the above work of Lin et al.,¹² to our knowledge, the use of nonsolvents for studying organogels has not been reported so far. Among the polymers capable of forming thermoreversible organogels, poly(methyl methacrylate) (PMMA) presents advantages such as transparency and biocompatibility which are the desired properties for the applications of a porous structure. We are unaware of any report on the preparation of porous PMMA gel via the nonsolvent method.

Thermoreversible gel systems swollen in a liquid are usually very brittle. Their structure is physically cross-linked by weak forces (e.g., Columbic, hydrogen bond, and van der Waals).¹³ Generating porosity induces a complex microstructure which shows poor mechanical performance. To overcome this problem, we explored nanocomposite systems composed of PMMA gels and carbon nanotubes (CNT). Polymer nanocomposites are a new and fast-growing class of polymer materials. The concept to

*Corresponding author. E-mail: Sundar@Carleton.ca.

(1) Rao, C. N. R. *J. Mater. Chem.* **1999**, *9*, 1–14.

(2) Hikmet, R. M.; Callister, S.; Keller, A. *Polymer* **1988**, *29*, 1378–1388.

(3) Vandeweert, P.; Berghmans, H.; Tervoort, Y. *Macromolecules* **1991**, *24*, 3547–3552.

(4) Tsai, F.-J.; Torkelson, J. M. *Macromolecules* **1990**, *23*, 775–784.

(5) Cheng, J. M.; Wang, D. M.; Lin, F. C.; Lai, J. Y. *J. Membr. Sci.* **1996**, *109*, 93–107.

(6) (a) Antonietti, M.; Caruso, R. A.; Goltner, C. G.; Weissenbag, M. C. *Macromolecules* **1999**, *32*, 1383–1389. (b) Dasgupta, D.; Nandi, A. K. *Macromol. Symp.* **2007**, *251*, 15–24.

(7) Tokuyama, H.; Kaenohara, A. *Langmuir* **2007**, *23*, 11246–11251.

(8) Kato, N.; Takahashi, F. *Bull. Chem. Soc. Jpn.* **1997**, *70*, 1289–1295.

(9) Tokuyama, F.; Masada, I.; Shimamura, K.; Ikawa, T.; Monobe, K. *Colloid Polym. Sci.* **1986**, *264*, 595–601.

(10) Ceylan, D.; Okay, O. *Macromolecules* **2007**, *40*, 8742–8749.

(11) Mulder, M. *Basic Principles of Membrane Technology*, 2nd ed.; Kluwer Academic Publishers: Dordrecht, 1996. Kuo, C.-Y.; Su, S.-L.; Tsai, H.-A.; Su, Y.-S.; Wang, D.-M.; Lai, J.-Y. *J. Membr. Sci.* **2008**, *315*, 187–194. Kuo, C. Y.; Lin, H. N.; Tsai, H. A.; Wang, D.-M.; Lai, J.-Y. *Desalination* **2008**, *233*, 40–47. McKelvey, S. A.; Koros, W. J. *J. Membr. Sci.* **1996**, *112*, 29–39.

(12) Lin, K.-Y.; Wang, D.-M.; Lai, J.-Y. *Macromolecules* **2002**, *35*, 6697–6706.

(13) Almdal, K. *Polym. Gels Networks* **1993**, *1*, 5–17.

combine an organic matrix with CNT is expected to lead to an improvement of the mechanical and thermal properties of the polymer phase. Since their discovery by Iijima,¹⁴ CNTs have sparked an overwhelming interest in the development of new nanocomposite materials. Because of their high aspect ratio, mechanical strength, and high modulus,¹⁵ CNTs are an interesting candidate to toughen a gel structure. It was shown that the incorporation of CNT's enhances the properties of hydrogels of alginate¹⁶ and alanine.¹⁷

In this paper, we report a new and simple method, based on PMMA gelation in the presence of carbon nanotubes, which allows synthesizing porous PMMA gels with reinforced structure. Our strategy to generate porosity is based on the incorporation of a nonsolvent for PMMA (water or an organic solvent) before the gelation process. We believe that this is the first report of a porous polymer gel incorporating CNT. The effects of different nonsolvents and CNTs concentration on the gel morphology have been investigated.

Experimental Part

Materials. Poly(methyl methacrylate) (PMMA) ($M_w = 350\,000 \text{ g mol}^{-1}$) was purchased from Aldrich Chemical Co. and was used as received. The single-walled carbon nanotubes were purchased from CarboLex (Batch CLAP8333) and were purified following the procedure described in our earlier publication.¹⁸ The CNTs were purified by refluxing with 35% HNO₃ for 24 h followed by repetitive washing with distilled water and centrifuging until a neutral supernatant was obtained. These CNTs tend to bundle into ropes with an average diameter of about 30.5 nm measured from the scanning electron microscopy. The SEM micrograph and size distribution histogram of the purified CNTs are given in the Supporting Information (Figure S1). Acetone (Fisher scientific), methanol (Caledon), and cyclohexane (Caledon) were used as received.

Fabrication of PMMA Gels (Protocol 1). PMMA (0.25 g) was dissolved in 2 mL of acetone (i.e., 15% in weight) in a closed vial under magnetic stirring and heating (55 °C). Then the vial was quenched in a bath of dry ice and acetone (−70 °C) for 10 min. The gel so formed was stabilized by evaporation of the supernatant. The same protocol was carried out for the synthesis of PMMA gels in the presence of CNT (CNT–PMMA gel) using a dispersion of CNT in acetone.

Fabrication of Porous PMMA Gel (Protocol 2). PMMA (0.25 g) was dissolved in 2 mL of acetone (i.e., 15% in weight) in a closed vial under magnetic stirring and heating (55 °C). Then, the desired amount of nonsolvent (water, from 15 to 25% in volume compared to acetone) was added dropwise to the mixture under stirring, inducing polymer precipitation. At this stage, the polymer precipitate was dissolved back by briefly increasing the temperature of this system (solvent, nonsolvent, polymer precipitates) to 90 °C while stirring in the closed vial. The dissolution was rapid. Then the vial was quenched in ice for 10 min to produce the porous gel (H₂O–PMMA gel). The gelation was instantaneous and stable at room temperature.

Fabrication of Porous PMMA/CNT Nanocomposite Gel (Protocol 3). CNT (from 0.25 to 1 wt % of PMMA) was dispersed in the nonsolvent by sonication (Branson 1510, frequency 40 kHz) for 2 h. PMMA solution was prepared following the previous procedure under magnetic stirring and

heating. Then the CNT dispersion in the nonsolvent was added to the solution drop by drop, and the polymer precipitated. It was dissolved back by briefly heating to 120 °C in a closed vial while stirring. The dissolution was rapid. The new solution was quenched in ice for 10 min to produce the porous PMMA/CNTs nanocomposite gel.

Morphology. The wet gel was cut into pieces using a sharp blade and was kept at room temperature in the fume hood to let the solvent evaporate. The dried gel so formed was studied by scanning electron microscopy (SEM, JEOL JSM-6460 microscope) through their cross-sectional view. Dried gel samples were coated with gold (80%) and palladium (20%) alloy layer by Hummer VII sputtering system (Anatech Ltd., Alexandria, VA) under argon to make them conductive. The thickness of conductive layer was 9–10 nm. The pore size distributions of the gels were then measured from the SEM images using Northern Eclipse image processing software. In each case, an area of 115 μm × 155 μm of the cross-sectional area was chosen. The perimeters, rather than radii, were measured due to the different shapes of the pores.

Stretching Test. Uniaxial stretching test was carried out with a hand-held stretcher (shown in Figure S2) having 1.55 mm progress per load cycle to determine the elastic property of the gels. A small piece of undried gel sample having approximate dimension of 1 cm in length, 0.2 cm in width, and 0.75 mm in thickness was stretched slowly from an initial length L_0 to a length L until break. Five samples were used in each case. The elongation ratio (λ) was calculated with the following expression:

$$\lambda = (L - L_0)/L_0 \quad (1)$$

Spectroscopy. FTIR spectra of the neat CNT, PMMA, and the composite gels were taken under ambient conditions with a Varian 1000 Scimitar Series spectrophotometer equipped with an attenuated total reflectance (ATR) setup. The FTIR spectra were recorded using as-prepared, completely dried samples with a background correction using the identical sample holder. Varian Resolution (version 4.0.5.009) software was used to process the data.

Raman spectra were collected in a single-stage spectrophotometer equipped with a liquid nitrogen-cooled CCD camera (Princeton Instruments). Excitation was provided by an Ar ion laser (Coherent, Innova 70C Spectrum) operating at 488 nm. A notch filter was used to remove the excitation background. Cyclohexane was used for Raman shift calibration. The spectral resolution of the instrument was 4 cm^{−1}. Spectra were processed using GRAMS/AI (Thermo Galactic) software.

Results and Discussion

As described in the previous section, four types of gels have been prepared for this study: (1) PMMA gel in acetone without any porogens (nonsolvent) or fillers (CNT), (2) PMMA gel in the presence of CNT (CNT–PMMA gel), (3) PMMA gel in the presence of water (H₂O–PMMA gel), and (4) PMMA/CNT nanocomposite gels which were prepared in the presence of both water (nonsolvent) and CNT.

Origin of the Porosity. Figure 1 shows the SEM images of the first three types of PMMA gels. The PMMA gel in acetone (Figure 1a) presents a smooth surface, and no pores are observed. This is in contrast to the observations of Vandeweerdt et al.³ and Tsai and Torkelson,⁴ who used solvents such as 1-butanol, cyclohexanol, and sulfolane. The nonporous morphology characterizes the CNT–PMMA samples as well (Figure 1b). Thus, the CNT by itself does not act as a porogen in this case. Figure 1c shows the SEM images of the H₂O–PMMA gel (without CNT) exhibiting high concentration of pores with a distribution of sizes. Some are about 10 μm in diameter, and others are quite elongated.

(14) Iijima, S. *Nature (London)* **1991**, *354*, 56–58.

(15) Saito, R.; Dresselhaus, G.; Dresselhaus, M. S. *Physical Properties of Carbon Nanotubes*; Imperial College Press: London, 1998 (ISBN: 1-86094-093-5).

(16) Ma, L.; Wen, J. *Compos. Sci. Technol.* **2008**, *68*, 1297–1303.

(17) Pal, A.; Chhikara, B. S.; Govindaraj, A.; Bhattacharyya, S.; Rao, C. N. R. *J. Mater. Chem.* **2008**, *18*, 2593–2600.

(18) Singh, S.; Pei, Y.; Miller, R.; Sundararajan, P. R. *Adv. Funct. Mater.* **2003**, *13*, 868–872.

Thus, the porosity is generated by the incorporation of water before gelation. Indeed, PMMA is not hydrosoluble, and it precipitates and traps water in its structures, creating cavities after gelation and evaporation. Water acts as a porosity generator which is simply removed by evaporation from the gel sample. This phenomenon of organogelation in the presence of nonsolvent (water) is limited in range, as shown in Figure 2. We found that the lower limit of spontaneous gelation corresponds to a water concentration of 15% in volume with respect to acetone, irrespective of the concentration of PMMA. Below this water concentration, no gelation that is stable at room temperature occurs as seen in Figure 2c. The upper limit of water concentration

is 25% in volume. Above this limit, PMMA did not dissolve in the solvent mixture of acetone and water.

Apart from water, other nonsolvents for PMMA which are miscible with acetone were also used with acetone to prepare gels (ns-PMMA gel), following the same protocol as for water. Figure 3 shows the SEM images of gels made using acetone with methanol, propanol, and cyclohexane as the nonsolvents. They all exhibit porous morphology, which shows that porosity could be generated, not only by water but also by other organic solvents provided that they are miscible with acetone and are nonsolvents for PMMA. The only difference between water and the other organic nonsolvent systems is the limits of spontaneous gelation. While water addition induces stable gels from 15% (v/v), the lower limit of gelation for other organic nonsolvents is higher. We observed that gelation starts from 50% (v/v) for methanol and cyclohexane and 75% (v/v) for propanol.

We attempted to qualitatively rationalize the porosity with the solubility of the polymer. The solubility parameters δ of PMMA and acetone are about the same ($19\text{--}20 \text{ MPa}^{1/2}$). The δ is much higher for water ($48 \text{ MPa}^{1/2}$), Methanol ($29 \text{ MPa}^{1/2}$), propanol ($24.9 \text{ MPa}^{1/2}$), and cyclohexane ($16.8 \text{ MPa}^{1/2}$) exhibit quite different solubility parameters. We can calculate the solubility parameter δ of the solvent mixture (near the lower limit of gelation) by averaging the δ value of the individual solvents by volume. Thus, the δ of water-acetone (15/85), methanol-acetone (50/50), propanol-acetone (75/25), and cyclohexane-acetone (50/50) mixtures are about 23.9, 24.4, 22.9, and $18.3 \text{ MPa}^{1/2}$, respectively. Note that in Figure 3 images a, b, and c are in decreasing order of the solubility parameter δ . It is seen that the pores in Figure 3a (with methanol/acetone, highest δ 's of mixtures) are large and irregular. They become more uniform in the case of propanol/acetone with a smaller δ . As the δ decreases further, in the case of cyclohexane as the nonsolvent, the pores are smaller, and most of them are very uniform in size. The histogram in Figure 3 shows that the pores in the gel made with cyclohexane are uniform in size, with an average of $25 \mu\text{m}$ in perimeter. Those from methanol and propanol show larger pores with a wide distribution. Thus, we formed porous gels by using a solvent

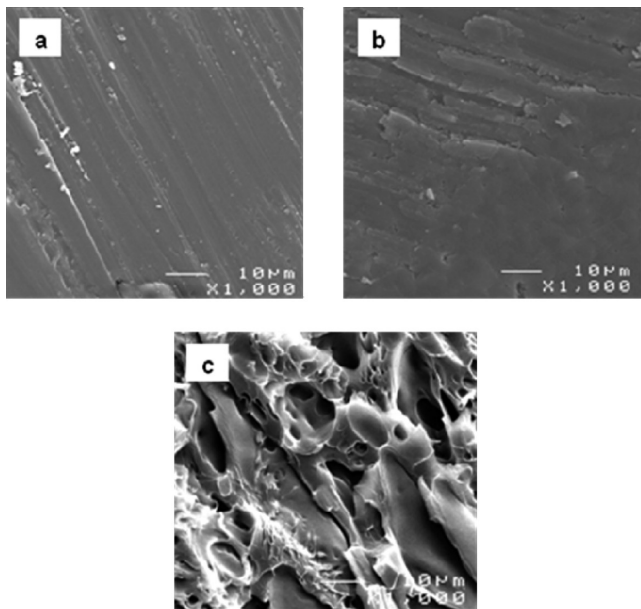
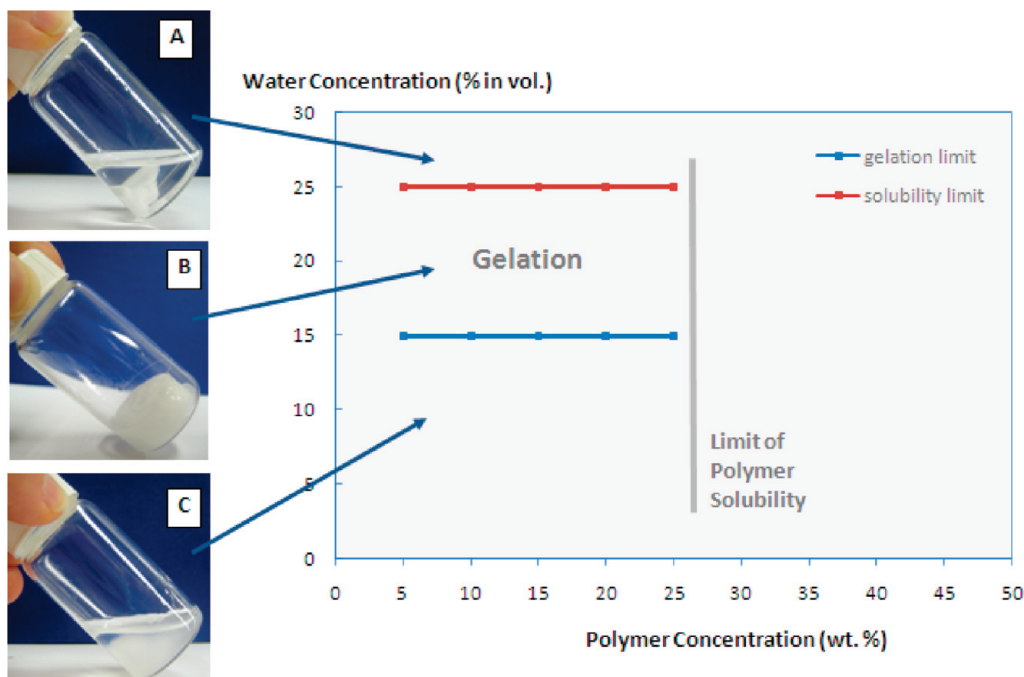


Figure 1. SEM micrographs of (a) PMMA gel, (b) CNT-PMMA gel containing 0.5 wt % CNT, and (c) H_2O -PMMA gel containing 15% (v/v) of water.



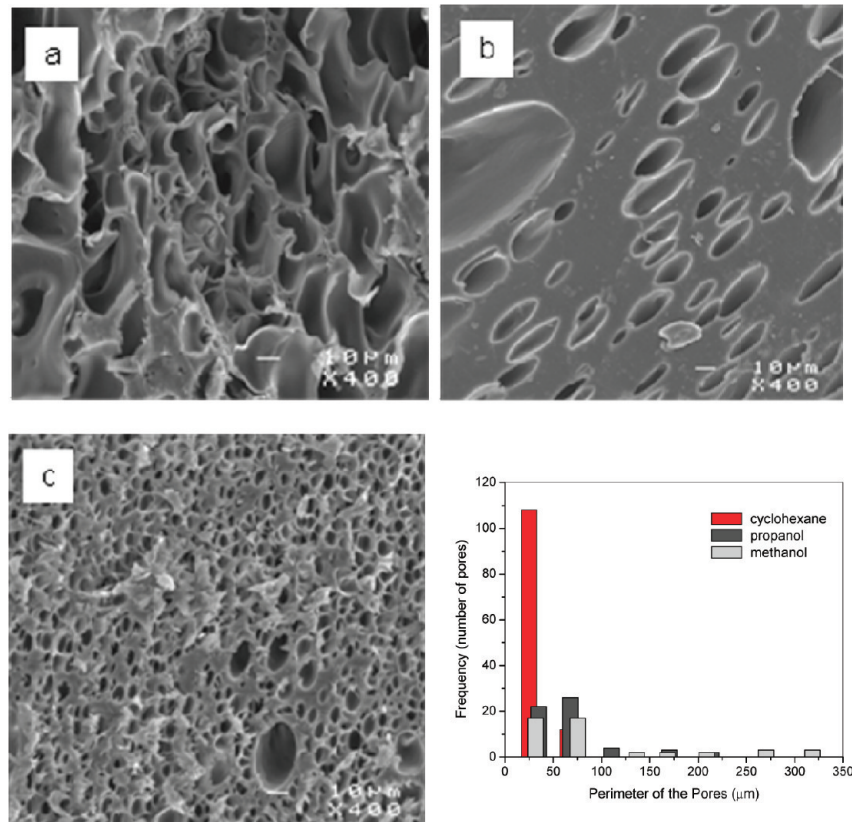


Figure 3. SEM micrographs of nonsolvent-PMMA gel samples with ns: (a) methanol, (b) propanol, and (c) cyclohexane. The histogram shows the pore size distribution of the gels.

mixture with a δ close to that of PMMA and using a nonsolvent as a porogen. If the relationship between δ and the porosity is applicable broadly, the nonsolvent route used here offers some control over the pore size. The method described by Vandeweerdt et al.³ and Tsai and Torkelson⁴ is different since they used a solvent with much higher δ than PMMA.

PMMA/CNT Nanocomposite Gels. Porous nanocomposite gels, in the presence of water and CNT, were prepared following the protocol 3. The incorporation of the CNT in H₂O-PMMA gels has a direct impact on their morphologies. Figure 4 allows a comparison of morphologies of samples without the CNT and nanocomposite samples with CNT, with the same proportion of water. At low concentration of the nonsolvent (15%), the CNT-free sample exhibits a high porosity (Figure 4a₁₅) with large and connected cavities. The morphology of the corresponding nanocomposite sample (Figure 4b₁₅) is quite different. The pores are smaller and more regular. As seen from the histogram (Figure 4C₁₅), the gel with CNT shows small and uniform pores, with the major distribution around 25 μm. The pores are with wider distribution without the CNT (note the red bar behind the black bar centered at 25 μm in this figure). The same trend was observed at higher proportion of nonsolvent. Figures 4a₂₀ (CNTs free), 4b₂₀, and 4C₂₀ correspond to 20% H₂O-PMMA gel. Once again, the morphology of the CNT-free gel (with spherical and large pores) is modified by incorporation of CNTs. The nanocomposite sample exhibits fewer large pores.

Two sets of nanocomposite gels with CNT concentration ranging from 0.25% to 0.75% were prepared to compare their morphology and determine the effect of CNTs concentration on the porosity. The amount of water was set at 15% and 25% for parts a and b of Figure 5, respectively. The corresponding histograms of pore size distribution are shown in parts C₁₅ and

C₂₅ of Figure 5, respectively. The same trend in term of porosity is observed for both sets. At low concentrations of CNTs, in addition to small pores of about 20–25 μm, a few with large perimeters (60–120 μm) are also seen (Figures 5a₁ and 5C₁₅). The pore size decreases with an increase in the CNT concentration, with no large pores with a CNT concentration of 0.75%. Whatever the initial concentration of nonsolvent, the addition of CNTs leads to a reduction of the pore size in the nanocomposite gel.

Influence of CNTs as Nanocomposite Fillers. CNT as a component of nanocomposite gels is expected to enhance the mechanical or rheological properties. A few simple experiments were performed to determine the influence of CNTs in term of physical properties. Uniaxial stretching test was carried out using a manual stretcher. The elongation ratios are listed in Table 1. PMMA gel and H₂O-gels without any CNTs exhibit a low capacity for elongation between 3.9 and 6.6. Table 1 shows that the elongation ratios of the nanocomposite gels, with CNTs as fillers, are twice those of the gels without. Irrespective of the initial concentration of water, increasing the CNT content in the gels results in a higher elongation ratio. This trend is almost linear and indicates the direct impact of CNT on gel mechanical properties. When a porous structure undergoes elongation or compression, the pores weaken in structure and could be the origin of crack leading to the failure of the gels. In our nanocomposite gels, we suggest that CNTs create a solid network within the polymer. Because of their excellent mechanical properties, they can limit the crack propagation and reinforce the gel structure. In order to confirm these assumptions, all stretched samples were dried and their morphologies were studied by SEM and compared to CNT-free samples (H₂O-PMMA gels) after stretching.

The nanocomposite gel was stretched slowly and slightly only to thin its structure. The stretching pressure was maintained

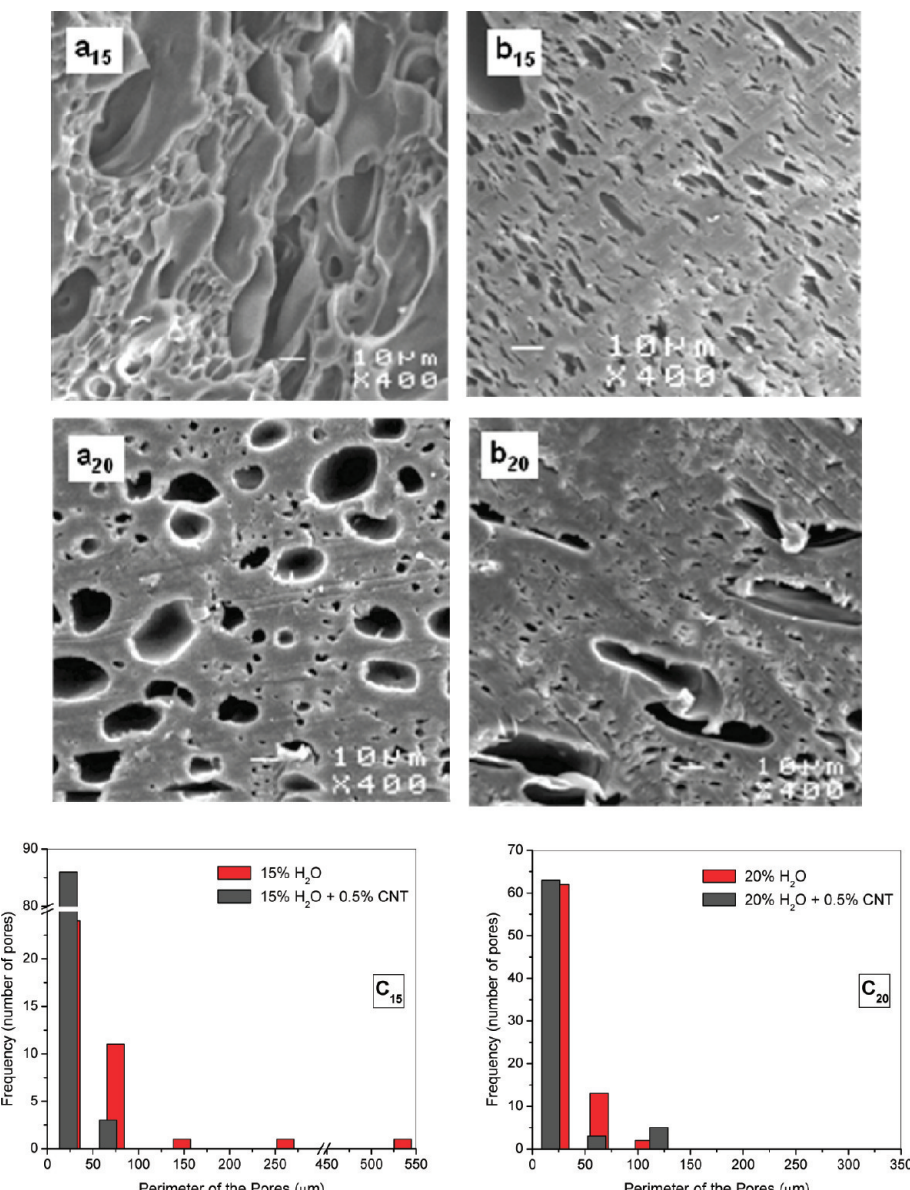


Figure 4. SEM micrographs of H₂O-PMMA gels (i.e., CNTs free samples) (**a**₁₅, **a**₂₀) and CNT-PMMA nanocomposite gels (**b**₁₅, **b**₂₀) with 0.5 wt % of CNT. The numbers 15 or 20 indicate the concentration of water (15% or 20% (v/v)) added before gelation. Histograms **C**₁₅ and **C**₂₀ show the pore size distributions of the gels prepared without and with 0.5% CNT using 15% and 20% H₂O as nonsolvent, respectively.

during the evaporation of the solvent to conserve the gel structure. Figure 6 shows that in this stretched sample with porous morphology CNTs are concentrated in or on the pore walls (the tips of these are marked by arrows in Figure 6a). The micrograph at higher magnification (Figure 6b) confirms the presence of CNTs in the pores. The arrows point to thin wires, which represent the CNT covered by the polymer. It is also seen that with this minimal stretching Figure 6b shows filament-like morphology. Thus, this experiment, at low elongation, indicates the presence of concentrated CNT zone around the pores. Note that the porous morphology is obtained when water is added. The CNT is also dispersed in water.

To further show that the CNT forms a network, the nanocomposite gels were stretched almost up to their break point. These were then kept in the stretched state during solvent evaporation. The dried samples were carefully washed with a few drops of acetone to dilute PMMA layer and make CNTs more observable in SEM. Figure 7 shows the micrographs for the CNT-free (porous, however) and CNT nanocomposites.

Figure 7a,b shows that before acetone treatment no significant difference is visible between the CNT-free (Figure 7a) and the nanocomposite gels. However, the SEM micrograph (Figure 7b_w) of the nanocomposite gel after solvent washing exhibits a well-defined and homogeneous CNT network. Thus, acetone treatment allowed us to reduce the polymer layer and observe the CNT network. The same treatment was also applied to CNT free sample. Its morphology (Figure 7a_w) was not significantly affected by the solvent washing. Thus, we have shown that CNT, dispersed in water and then added to PMMA solutions, creates a solid network within the porous polymer matrix of the nanocomposite gels and plays an important function during samples stretching. This is similar to the network seen with PMMA-CNT nanocomposite films prepared by Du et al.¹⁹ using a coagulation method as well as with the polycarbonate-CNT composites.¹⁸ During stretching, pores are source of cracking and weakening

(19) Du, F.; Scogna, R. C.; Zhou, W.; Brand, S.; Fischer, J. E.; Winey, K. I. *Macromolecules* **2004**, *37*, 9048–9055.

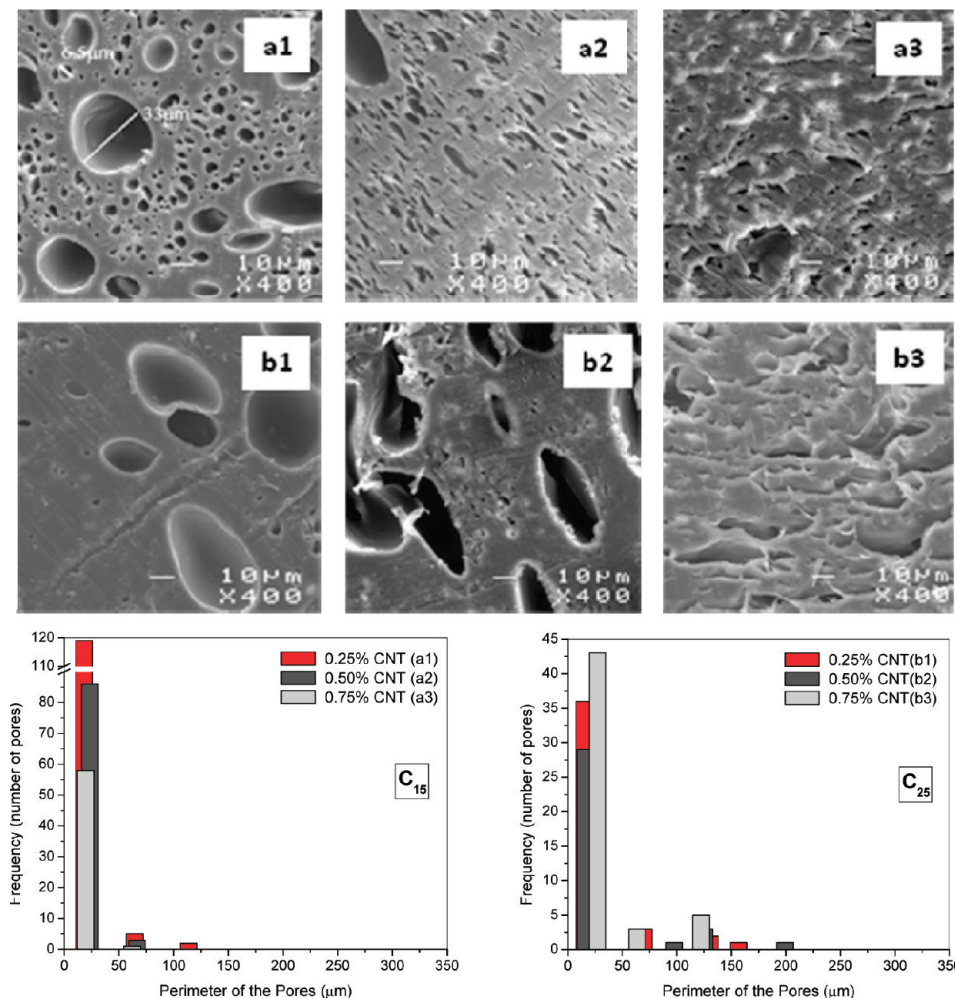


Figure 5. SEM micrographs of CNTs-PMMA nanocomposite prepared with 15 (a1, a2, a3) and 25 (b1, b2, b3) (v/v) % of water. The numbers 1, 2, and 3 indicate the amount of CNTs 0.25; 0.5; 0.75 wt % respectively, in the nanocomposite. Histograms C₁₅ and C₂₅ show the pore size distribution of the gels with corresponding CNT loading prepared with 15 and 25% H₂O as nonsolvent, respectively.

Table 1. Elongation Ratios of H₂O-PMMA Gels and Nanocomposite Gels with Different Concentrations of Water and Carbon Nanotubes

CNTs (%)	water (%)			
	0	15	20	25
0	3.9 ± 0.5	4.5 ± 0.7	6.2 ± 0.6	6.6 ± 1.0
0.25		6.9 ± 2.0	7.8 ± 1.4	9.0 ± 1.5
0.50		8.7 ± 1.6	9.4 ± 2.2	10.8 ± 3.2
0.75		9.8 ± 0.5	11.3 ± 1.3	12.6 ± 2.0

the gel. A good network formation of CNTs around and in the pores as well as within the rest of the sample limits cracks from spreading over the gel structure.

Figure S3 shows CNT networks at different initial concentrations. Figure S3a is for the same sample as in Figure 7b_w in a different area. It is given here to compare the morphologies with different CNT concentrations. These are again the images recorded after washing with acetone. As expected, the more CNTs are incorporated in the gel, the better their network is developed and homogeneous. Such a network was seen throughout, and representative images are shown here. These observations are in line with values of elongation ratios presented before and confirm the important role of CNTs within the nanocomposite. Note that we added just a few drops of acetone to partially remove the PMMA to be able to see the CNT in

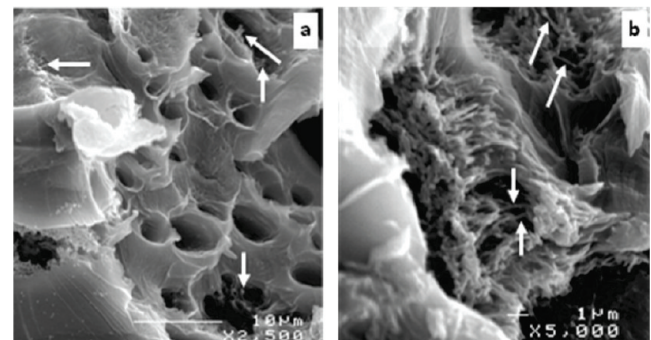


Figure 6. SEM micrographs of (a) low-stretched CNTs-PMMA nanocomposite gel and (b) zoom-in one of the pores. The concentrations of water and CNT are 15% (v/v) and 0.25 wt %, respectively.

Figures 7 and S3. The CNTs might still be covered by the polymer layer. In addition, the network appears dense in these figures, since the CNTs are mainly concentrated around the pores as mentioned above and as marked in Figure 6.

Spectroscopy of the CNT/PMMA Nanocomposite Gels. The possible interactions between the nanocomposite gel components were studied with two complementary spectroscopic techniques. Figure 8 shows the FTIR spectra of the neat components along with that of their composite gels. Neat PMMA

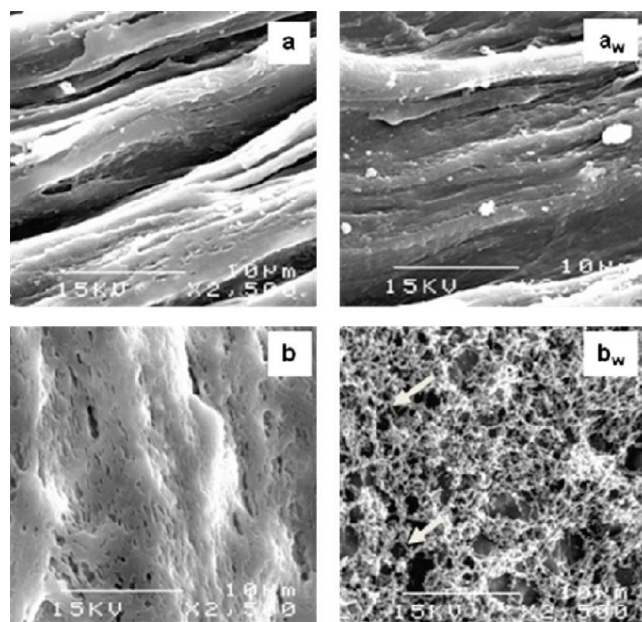


Figure 7. SEM micrograph of stretched (a) CNTs free and (b) nanocomposite samples. The letter w in indices indicates samples which have been washed by acetone. The concentrations of water and CNT are 15% (v/v) and 0.25 wt %, respectively.

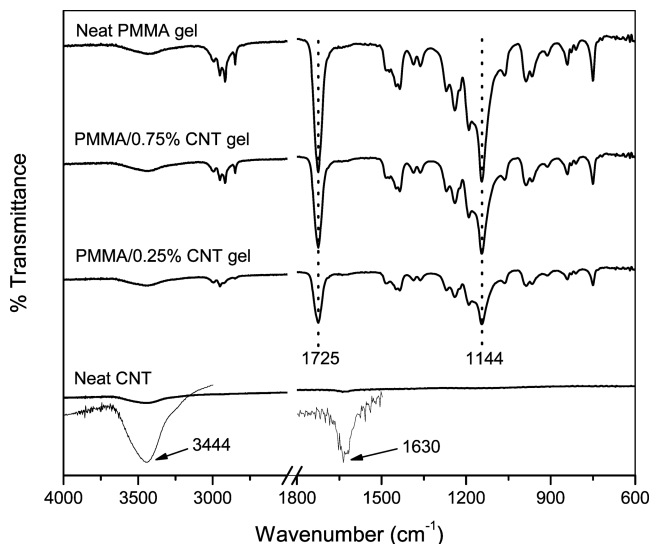


Figure 8. FTIR-ATR spectra of neat CNT, CNT/PMMA gels at 0.25% and 0.75% CNT loading, and the neat PMMA gels. The insets show the magnified view of the CNT spectra at those corresponding regions.

gel shows two strong absorption bands at around 1725 and 1144 cm^{-1} corresponding to C=O and C–O stretch of the ester group, respectively. Incorporation of CNT into the PMMA gels changes neither these band positions nor the spectral profile of the PMMA gel as evident from the composite gel spectra at different CNT concentrations. Neat CNT shows two significant absorptions in IR spectra at around 3444 cm^{-1} corresponding to the O–H, derived most probably from the oxidative purification of

(20) Lin, W.; Xiu, Y.; Jiang, H.; Zhang, R.; Hildreth, O.; Moon, K.-S.; Wong, C. P. *J. Am. Chem. Soc.* **2008**, *130*, 9636–9637. Kuhlmann, U.; Jantoljak, H.; Pfander, N.; Bernier, P.; Journet, C.; Thomsen, C. *Chem. Phys. Lett.* **1998**, *294*, 237–240. Kim, U. J.; Liu, X. M.; Furtado, C. A.; Chen, G.; Saito, R.; Jiang, J.; Dresselhaus, M. S.; Eklund, P. C. *Phys. Rev. Lett.* **2005**, *95*, 157402. Sbai, K.; Rahmani, A. H.; Chadi, H.; Bantignies, J.-L.; Hermet, P.; Sauvajol, J.-L. *J. Phys. Chem. B* **2006**, *110*, 12388–12393.

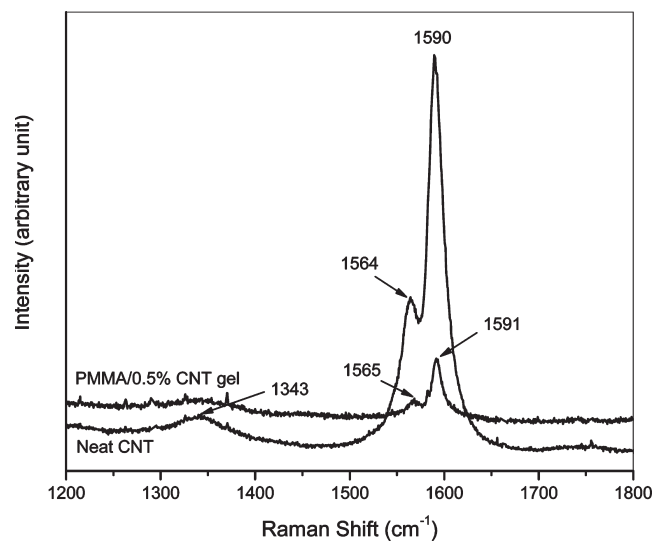


Figure 9. Raman spectra of neat CNT and CNT/PMMA composite gel.

CNTs, and at 1630 cm^{-1} , which could be attributed to O–H bending mode.²⁰ Neither of these inherently low intense absorption bands is visible in the composite gel spectra and probably smeared out due to the very low concentration of CNT in the composite gels. IR analysis clearly shows that the presence of CNT in the PMMA gel does not cause any change, derived from a chemical or nonbonded interaction, in its spectral profile. This can be attributed to both the very low extent of possible surface functionalization of CNTs during their oxidative purification process and very low concentration of the CNT in the gels. The reverse of this above-mentioned possibility, i.e., the influence of the major component PMMA on the minor component CNT, was studied with FT Raman spectroscopy. Figure 9 shows the Raman spectra of the neat CNT and the CNT/PMMA gel with 0.5% CNT load in the G and D band region. The Raman spectra of neat CNT shows typical G band at about 1590 cm^{-1} with a shoulder at the lower frequency end at about 1564 cm^{-1} . The so-called D band of CNT spectra indicative of defects and impurities^{21,22} also appeared at around 1343 cm^{-1} . The low intensity of D band compared to that of G band indicates a reasonably pure and defect free CNT sample²³ was used in this study. The Raman spectrum of the PMMA/0.5% CNT composite gel shows that there is no significant change in their peak position, which could otherwise mean an interaction between the components. The lower intensity of the bands can be attributed to the low concentration of CNT in the gel.

Conclusions

We have described the preparation of a novel porous PMMA thermoreversible gel with enhanced mechanical characteristics in the presence of carbon nanotubes. The gels were prepared from PMMA solution in acetone using a dispersion of CNTs in a nonsolvent (water). On the basis of porogen technology, nonsolvents were found to be responsible for the observed porosity and present the advantage that the porogen can be easily removed by simple evaporation. In addition, we have

(21) Marega, R.; Accorsi, G.; Meneghetti, M.; Parisinid, A.; Prato, M.; Bonifazi, D. *Carbon* **2009**, *47*, 675–682.

(22) Dresselhaus, M. S.; Dresselhaus, G.; Jorio, A.; Filho, A. G. S.; Saito, R. *Carbon* **2002**, *40*, 2043–2061.

(23) Arepalli, S.; Nikolaev, P.; Gorelik, O.; Hadjiev, V. G.; Holmes, W.; Files, B.; Yowell, L. *Carbon* **2004**, *42*, 1783–1791.

demonstrated that porosity can be designed according to the nature of the nonsolvent and its concentration. The simple protocol that we followed to incorporate CNT in PMMA gels using aqueous dispersions serves to create porosity as well as reinforce the pores though no chemical interactions between the components was evident from the spectroscopic analysis.

Acknowledgment. This work was supported in part by Natural Sciences and Engineering Research Council of Canada. M.V. also acknowledges the partial financial support from her

parents during the internship in Canada. We thank Dr. Anatoli Ianoul and Mr. Graham Galway of Carleton University for Raman spectroscopic analysis.

Supporting Information Available: SEM micrograph and size distribution histogram of the purified CNTs (Figure S1), the photograph of the hand-held device used for measuring elongation (Figure S2), and the SEM of the network morphology for different concentrations of CNT (Figure S3). This material is available free of charge via the Internet at <http://pubs.acs.org>.